

CHAPTER 4

A MICRO-ENZYME-IMMUNOASSAY FOR THE DETERMINATION OF THROMBOCYTE-ASSOCIATED IMMUNOGLOBULINS IN MALARIA PATIENTS

4.1 INTRODUCTION

Platelets (thrombocytes) are involved in the pathology of malaria as a result of their role in the immune response, especially in the inflammation reaction (1). Platelets, if not activated, are round or oval discs of about 2,8 μm in diameter. They originate from megakaryocytes in the red bone marrow and have granules that contain hormones, nucleotides, calcium, synthesized proteins and enzymes (2). The normal concentration of platelets in blood is between 150 000 and 350 000 per cubic millimeter. They possess class I MHC products and Fc receptors for IgG (Fc RIII) and IgE (Fc RII). Platelets can be sensitized via IgE binding of parasite antigens resulting in enhanced cytotoxicity against those parasites, as was illustrated with *T. gondii* and *T. cruzi* (3). Autoantibodies against platelets are seen in up to 70 % of cases of idiopathic thrombocytopenia. Removal of platelets is effected by splenic macrophages after infections or autoimmune diseases.

The surface of the cell membrane contains glycoproteins which adhere to damaged vessel walls. In addition, the membrane also has large amounts of phospholipids which can activate the "intrinsic" blood clotting system.

If the platelet count suddenly drops, recuperation will take about 5 days if the inhibiting agent is removed. Platelets have a half-life of 4 days and damaged or old platelets are sequestered in the liver and spleen. Besides their role in hemostasis, platelets protect the body against foreign invaders by immune adherence, removal from circulation and enhancement of phagocytosis.

Severe malaria infection is usually associated with thrombocytopenia, although the mechanisms underlying the reduced thrombocyte survival remain poorly understood (4). Strong evidence exists for an immunoglobulin mediated peripheral destruction, as increased levels of thrombocyte-associated immunoglobulins (TAIg) have been measured in malaria patients (5). Whether immunoglobulin binds to thrombocytes non-specifically by means of adsorption of immunoglobulins and immune complexes, or specifically by anti-thrombocyte auto-antibodies induced by the *Plasmodium* infection, is presently not known. Quantification of the immunoglobulins bound to thrombocytes is a necessary first step towards providing an answer to this question.

Several protocols for the determination of thrombocyte-associated immunoglobulins have been established since 1973 and were classified in three categories by Kelton (6). The so-called "two-stage assay" is best suited for the purpose of determining the specificity of binding of immunoglobulins to thrombocytes as it allows antibody displacement studies by cross-reactive antigens. Dixon *et al.* (7) pioneered the "two-stage assay" in 1975, using complement fixation to quantify the immunoglobulin. Nel and Stevens (8) improved this method in 1980, using serum-coated polystyrene balls in a more sensitive and less complicated

test tube ELISA to determine immunoglobulin concentration. The aim of the present study was to further improve this ELISA method by employing a transferable solid phase system (Nunc-TSP, trade mark) compatible for use with conventional microtitre plates. This modification avoids tedious washing of thrombocytes during the assay. Moreover, the two stages of the assay, viz. labelled antibody incubation with thrombocytes and determination of the remaining immunoglobulin, are combined in one step (Fig. 4.1), with considerable saving in time. The potential application of this assay method was demonstrated in four malaria patients with severe thrombocytopenia. High values of TAIg were demonstrated for these patients while insignificant levels of immunoglobulin were detected on thrombocytes of healthy blood donors or recovered malaria patients.

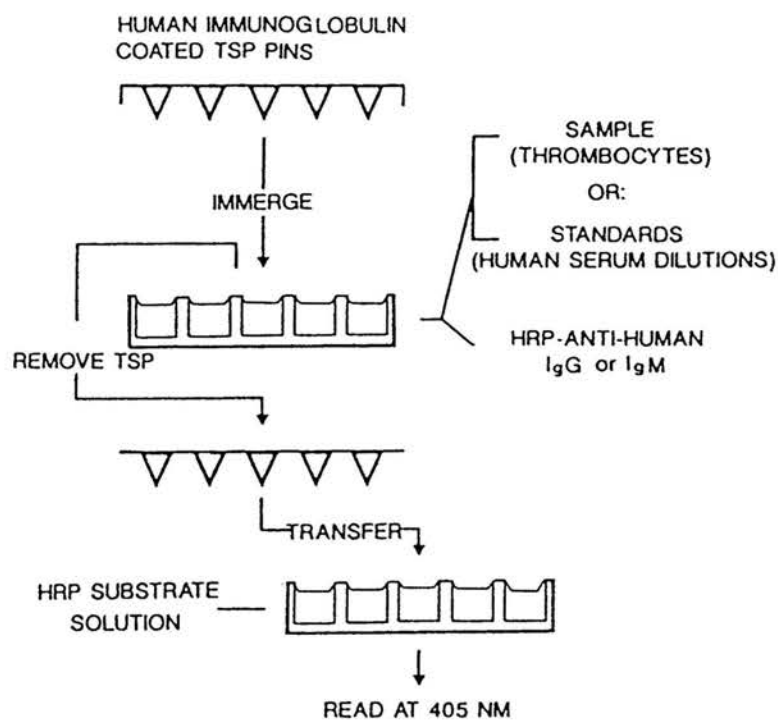


Figure 4.1 Diagrammatic presentation of the protocol for thrombocyte-associated immunoglobulin determination.

4.2 MATERIALS AND METHODS

4.2.1 Preparation of partially purified immunoglobulin.

Venous blood (500 ml) was collected in a blood collection bag without anti-coagulant and left at 4 °C overnight. The serum was separated from the clot by centrifugation at 1000 g on a Beckmann J6 centrifuge. Solid Tris was used to increase the pH of human serum to 8. While stirring, polyethyleneglycol (Fluka) was slowly added up to a concentration of 30 g/100 ml (9). The solution was left at 10 °C for 2 hours before collection of the precipitate by centrifugation (1000 g x 15 min). The precipitate was washed twice, dissolved in 30 ml borate-buffered saline (BBS) and lyophilized. The sample was later dissolved (BBS) and purified on a Sephacryl S.300 column in batches of 5 ml. Fractions (2.5 ml) were collected and tested by ELISA for the presence of IgG and IgM as follows: From each fraction 100 µl was dispensed in wells of a microtitre plate. After 2 hours of incubation at room temperature the samples were flicked out and the wells washed and blocked using 0.5 % (w/v) casein in phosphate-buffered saline pH 7.4. Rabbit anti-IgM and -IgG conjugated peroxidase (Cappel, Worthington) at 1/5000 dilutions were used to detect the presence of IgG and IgM in the fractions. Orthophenylene-diamine (1mg/ml) (Sigma, St. Louis, M.O.) and urea-hydrogenperoxide (0.6 mg/ml) in 0.1 citrate buffer, pH 4.5, was used as substrate solution (100 µl/well) and the colour change measured at 405 nm with a Titertek multiscan MC (Flow Labs Inc., Helsinki, Finland). All washing and blocking steps were carried out using 0.5 % casein/PBS.

4.2.2 Comparison between coating buffers and pin coating samples.

Coating of the pins with partially purified immunoglobulin or serum diluted in either 0.05 M glycine buffer (pH 2.7/7.4) containing 0.15 M NaCl or 0.1 M bicarbonate buffer, pH 9.3, were compared. The serum was serially diluted to give IgG and IgM concentrations of between 4 and 90 ug/ml in the coupling buffers. The partially purified immunoglobulin fractions were reconstituted to the same range of concentrations. The coating of the pins and the ELISA were done as described in 4.2.4 using different coating buffers and concentrations of serum or partially purified immunoglobulins.

4.2.3 Thrombocyte preparation.

Blood samples, collected from malaria patients and healthy volunteers with citric acid/ citrate/ dextrose as anti-coagulant, were donated by Dr Louis Marcus (Niehaus & Botha Pathologists, Pretoria). Patients were selected irrespective of the severity of infection or type and stage of treatment. Individuals selected as controls never had malaria and exhibited a normal thrombocyte count. Thrombocytes were isolated by differential centrifugation, washed with filter-sterilized phosphate-buffered saline (PBS), pH 6.5, and finally made up to 10^7 thrombocytes/ml in 0,5 % casein-PBS (pH 7.4). Thrombocytes were counted using an automatic thrombocytometer (Beckman).

4.2.4 Immunoglobulin coated TSP.

Polystyrene TSP pins (Nunc, Roskilde, Denmark) were coated with the purified immunoglobulin at 100 $\mu\text{g/ml}$ in glycine coating buffer (10) by incubation (5 hours, room temperature) of the TSP-pins in a pre-blocked microtitre plate filled with 200 $\mu\text{l/well}$ coating solution. Blocking was done

by incubation of plates or TSP-pins in 0.5 % casein/PBS for at least 3 hours (room temperature).

4.2.5 Determination of thrombocyte-associated IgG and IgM.

All washing of plates or TSP-pins and dilution of biological reagents were performed with 0.5 % casein/PBS. Wells of a pre-blocked microtitre plate were filled with 100 μ l of a dilution range of standard human serum (Hoechst-Behring; France) to obtain a standard curve of either IgG or IgM of 0-100 ng/well. The remaining wells received 100 μ l of thrombocyte suspension samples from patients and healthy controls at 10^6 thrombocytes per well. Depending on whether IgG or IgM was determined, horse radish peroxidase conjugates of either sheep anti-human IgG (1:3000) or sheep anti-human IgM (1:2000) (Cappel, Worthington) were added at 100 μ l per well prior to the immersion of the coated TSP-pins into the wells. After incubation for 3 hours at room temperature in a plate shaker, the TSP-pins were removed, washed and transferred to a microtitre plate filled with substrate solution (100 μ l/well) consisting of orthophenylenediamine (1 mg/ml) (Sigma, St. Louis, M.O.) and urea-hydrogenperoxide (0,6 mg/ml) in 0.1 M citrate buffer, pH 4.5. Colour development was measured at 405 nm with a Titertek Multiscan MC.

4.3 RESULTS

4.3.1 Preparation of partially purified immunoglobulin.

Polyethylene glycol (PEG) selectively precipitated the serum proteins depending on their molecular size and concentration. Using 30 % (w/v) PEG, most of the larger serum proteins were precipitated. To evaluate

the fraction collected, a sample was separated on Sephachryl S-300 and eluted fractions screened by ELISA for the presence of IgG and IgM. In Fig. 4.2 typical results are shown.

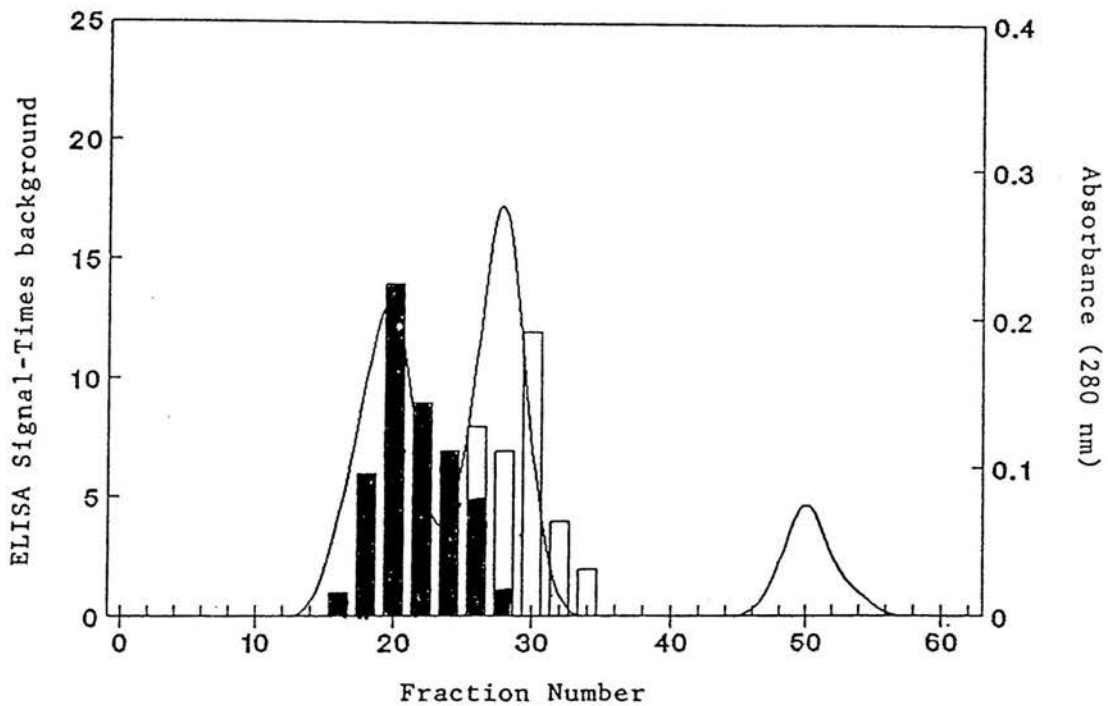


Figure 4.2 Elution pattern of the immunoglobulin fraction isolated from human serum on a 40x1.5 cm Sephacryl S-300 column. Flowrate was 0.5 ml/min and 2.5 ml fractions were collected. The ELISA signal is given as multiple of background measured at 405 nm. Fractions 15 to 30 showed IgM activity and fractions 23 to 35 exhibited IgG activity.

■ IgM
 □ IgG

Fractions 15 to 36 were pooled, lyophilized and used as the partially purified immunoglobulin fraction.

4.3.2 Coating buffers and immunoglobulin source for coating pins.

Glycine and bicarbonate buffers were compared using serum and a partially purified immunoglobulin fraction as coating samples for TSP pins. The results for IgG and IgM are shown in Figs 4.3 and 4.4, respectively.

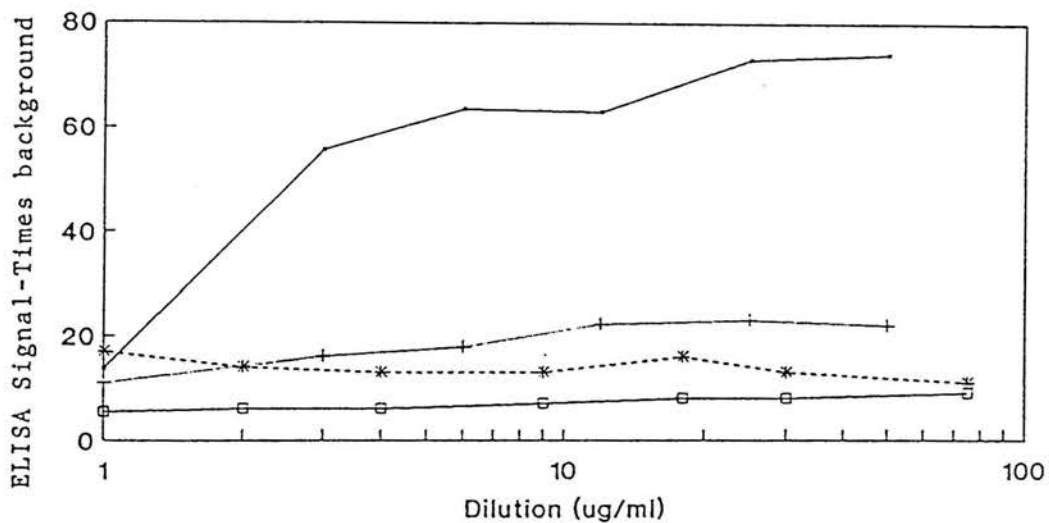


Figure 4.3 Comparison between coupling methods for IgG.
 (a) Partially purified IgG/M coating with glycine coating buffer —
 (b) Partially purified IgG/M coating with carbonate coating buffer —+
 (c) Serum coating with glycine coupling buffer ---*--
 (d) Serum coating with carbonate coupling buffer —e—

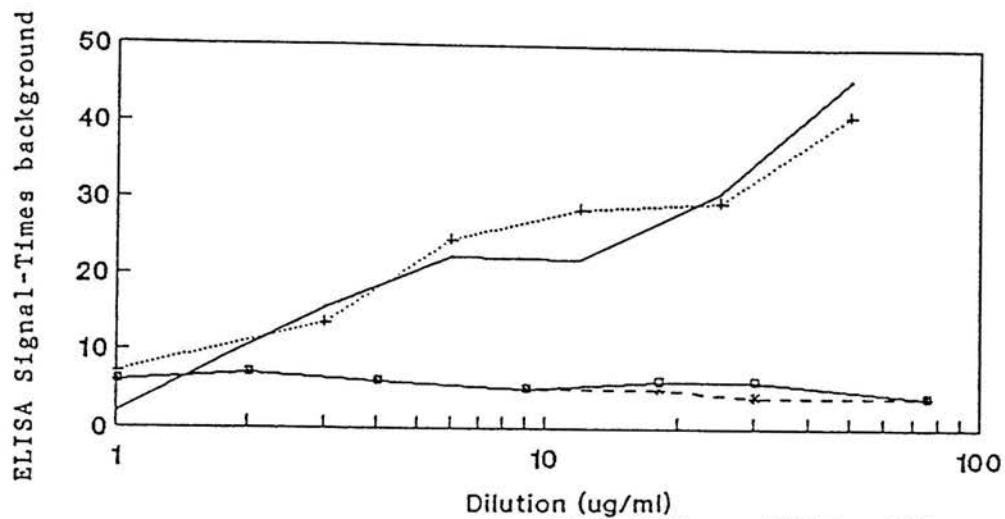


Figure 4.4 Comparison between coupling methods for IgM.
 (a) Partially purified IgG/M coating with glycine coating buffer —
 (b) Partially purified IgG/M coating with carbonate coating buffer —+—
 (c) Serum coating with glycine coating buffer ---*---
 (d) Serum coating with carbonate coating buffer —□—

From these results it is evident that partially purified IgG coated with glycine buffer generates higher signals than serum, or partially purified IgG coated with the carbonate buffer. Coating the partially purified fraction in either the glycine, or carbonate buffer generated equally good signals for IgM, while unpurified serum did not yield satisfactory results with either buffer system. The glycine buffer system therefore was used as coating buffer and partially purified immunoglobulin fraction as the immunoglobulin source for coating the pins in the assay.

4.3.3 Optimization of the coupling of immunoglobulins onto TSP-pins.

The ELISA signals obtained when using different concentrations of immunoglobulin for coating TSP-pins in an assay where thrombocytes or standard serum was omitted, are represented in Fig. 4.5. IgG produced

approximately a two-fold stronger signal than IgM, but both approached saturation at 200 $\mu\text{g/ml}$ coating concentration.

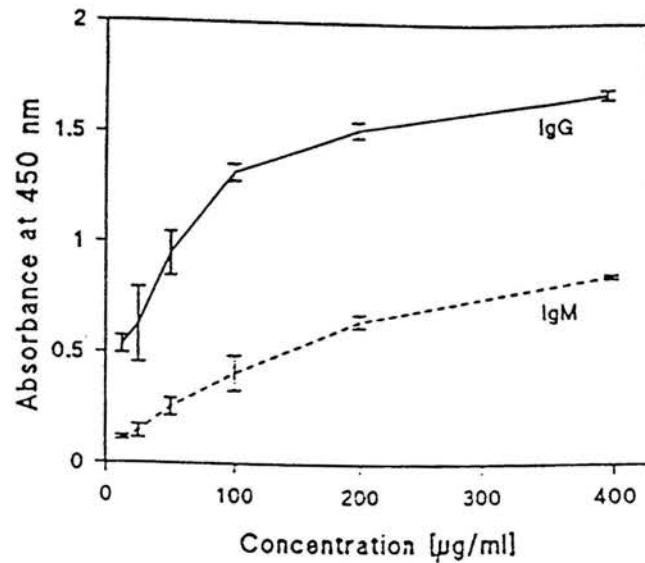


Figure 4.5 Optimization of the coupling of partially purified immunoglobulin onto the TSP-pins.

4.3.4 Standard curves.

A critical parameter determining the sensitivity of the assay, is the dilution of peroxidase-conjugate used as indicator. A dilution-response curve was obtained by titration of the indicator reagent, to determine the first order region. From the results in Fig. 4.6, values of 1:2000 for anti-IgM-and 1:3000 for anti-IgG-peroxidase were selected for the assay, as they occur in the first order region, generating a sufficient ELISA signal.

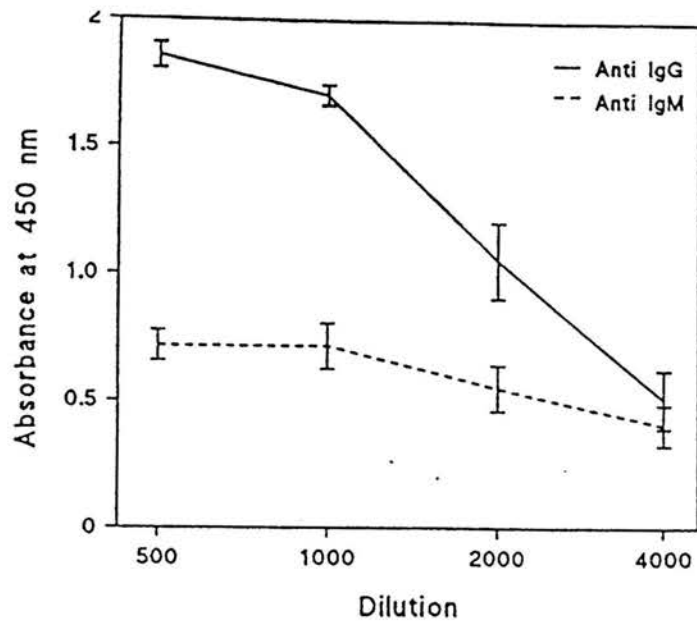


Figure 4.6 Optimization of the dilution of anti-IgG and -IgM-peroxidase.

Using these optimal dilutions of indicator antibody, standard curves for IgG and IgM were obtained by using standard human serum to inhibit binding of the former to the TSP-pins (Fig. 4.7 and 4.8).

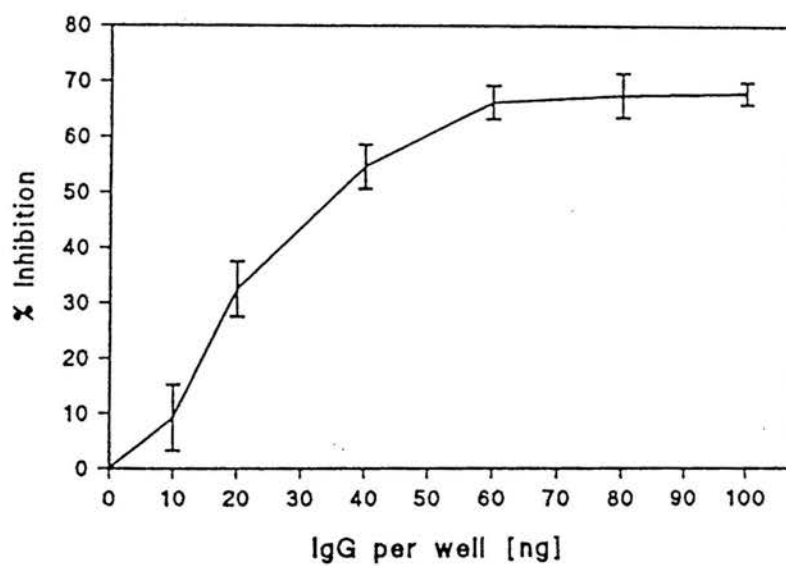


Figure 4.7 Standard curve for the quantification of TAIgG.

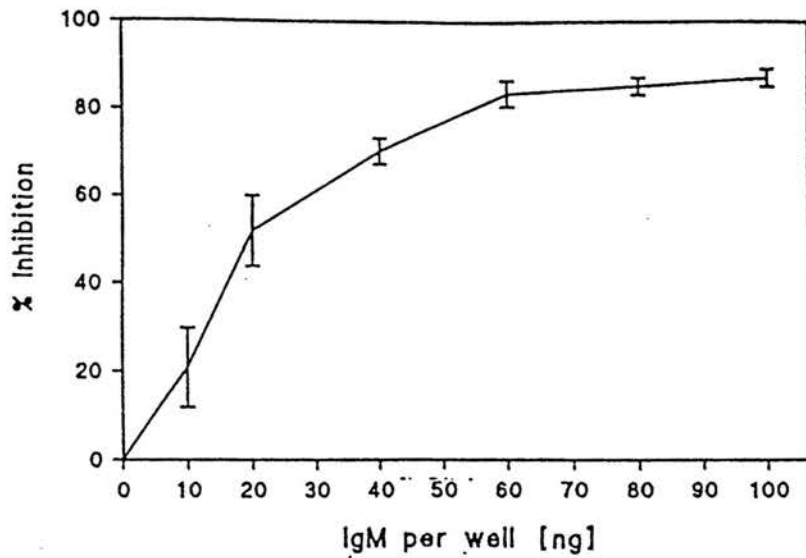


Figure 4.8 Standard curve for the quantification of TAIgM.

A linear response was obtained in the range of 0-20 ng per well for both IgM and IgG, rendering the assay useful for the determination of 5-50 ng of IgG or IgM.

4.3.5 Measurement of thrombocyte-associated IgG and IgM.

Results for 15 measurements of thrombocyte-associated immunoglobulins G and M, including four healthy controls, are summarized in Table 4.1.

Table 4.1. ELISA determination of thrombocyte-associated IgM (TAIgM) and IgG (TAIgG) in human blood.

Source of blood samples†	Thrombocyte count ($\times 10^9/l$)	IgM*		IgG*	
		ELISA signal inhibition (%)	TAIgM (ng/ 10^6 thrombocytes)	ELISA signal inhibition (%)	TAIgG (ng/ 10^6 thrombocytes)
Patient N	61	54	21 \pm 6	16	12 \pm 3
Patient G					
Day 0	54	57	26 \pm 4	71	>60
Day 1	48	89	>60	75	>60
Day 2	53	88	>60	73	>60
Patient H					
Day 0	72	75	48 \pm 5	26	17 \pm 2
Day 1	89	10	5 \pm 4	15	12 \pm 4
Day 2	113	2	2 \pm 4	15	12 \pm 2
Patient F					
Day 0	91	80	55 \pm 3	66	59 \pm 2
Day 1	108	32	14 \pm 4	61	52 \pm 2
Day 2	142	1	1 \pm 2	63	55 \pm 4
Day 3	211	0	0 \pm 1	20	15 \pm 4
Healthy individuals ($n=4$)	233 \pm 30	(-)5 \pm 6	0	(-)9 \pm 1	0

*Values represent the mean of 3 measurements.

†Days since start of anti-malaria chemotherapy are indicated.

In three malaria patients, blood samples were obtained for up to three successive days after malaria treatment commenced, which enabled us to relate recovery of the patient with platelet counts and the level of thrombocyte-associated IgG and IgM. A severe decreased platelet count was registered among all four malaria patients. An inverse correlation between thrombocyte count and thrombocyte-associated immunoglobulins was observed in respect to both IgM and IgG.

4.4 DISCUSSION

In preliminary studies where human α -globulin was bound to the bottom of ELISA plates instead of onto TSP-pins, high background values were obtained, which were not encountered by the TSP approach. While the approach of Nel and Stevens (8) required extensive washing of tubes and

α -globulin-coated balls during the assay to prevent the background problem, the unique geometry of the TSP system apparently escaped the effect of sedimenting immune complexes which non-specifically adsorb to bed surfaces. Fragmentation of the IgM fraction was observed in the elution pattern from the isolated human serum (Fig.4.2). This may have been due to the freezing and lyophilization of the PEG precipitate. However this will have no effect on the assay as only the heavy chain is recognized by the anti-IgM peroxidase.

The inverse correlation between thrombocyte count and thrombocyte-associated immunoglobulin IgM was previously described in respect of thrombocyte-associated IgG in mice with experimental malaria (11). The remarkably rapid recovery of thrombocyte count with concomitant loss of platelet-associated immunoglobulin argues against an active auto-immune mechanism in the complication of thrombocytopenia in cases of malaria. It would seem unlikely that auto-antibody secretion by active plasma cells could so suddenly be switched off after removal of the parasite antigens. A more tangible explanation of the results would be that the clearance of parasite antigen by chemotherapy reduces the immune complex load in the circulation and accordingly lifts the burden on the platelets, which normally are able to carry immune complexes via so-called complement receptors on their outer surface (12). No immunoglobulins could, however, be detected on thrombocytes of healthy individuals or a recently recovered malaria patient, e.g. "F" in Table 4.1. The results indicate that the detectability of the method developed suffices for determining levels of TA Ig typical of malarial thrombocytopenia. By using partially purified immunoglobulins a more sensitive method to that of Nel and Stevens is obtained (8). It requires relatively small volumes of blood

samples, comparable to the amounts required in the platelet-lysis method for TAIg determination developed by Hymes *et al.* in 1979 (13). The platelet-lysis approach, however, measures the total immunoglobulin found both inside and on the outer surface of the thrombocytes, which prevents its application to antibody displacement studies required for the specificity of TAIg.

4.5 REFERENCES

1. Roitt I.M., Brostoff J. and Male D.K. (1988). Cells involved in the immune response. In: Immunology (2nd Ed), Gower Medical Publishing, London, pp2.1- 2.17.
2. Grey S.V. and Meyer B.J. (1988). Die bloedplaatjies; homeostase. In: Die fisiologiese basis van geneeskunde. (Ed B.J. Meyer) 27.1-27.16, HAUM, Pretoria.
3. Roitt I.M., Brostoff J. and Male D.K. (1988). Immunity to Protozoa and Worms. In: Immunology (2nd Ed), Gower Medical Publishing, London, pp17.1-17.20.
4. Delgiudice, G., Grau, G.E., and Lambert, P.H. (1988). Host responsiveness to malaria epitopes and immunopathology. *Prog. Allerg.* 41, 288-330.
5. Kelton, J.G., Keystoke, J., Moore, J., Denomme, G., Tozman, E., Glynn, M., Neame, P.B. and Gauldie, J. (1983). Immune-mediated thrombocytopenia of malaria. *J. Clin. Invest.* 71, 832-836.
6. Kelton, J.G. (1983). The measurement of platelet-bound immunoglobulins: An overview of the methods and the biological relevance of platelet-associated IgG. *Prog. Hematol.* 13, 163-199.
7. Dixon, R., Rosse, W. and Ebbert, L. (1975). Quantitative determination of antibody in idiopathic thrombocytopenic purpura: correlation

- of serum and platelet-associated antibody with clinical response
Prog. J. Med. 292, 230-236.
8. Nel, J.D. and Stevens K. (1980). A new method for the simultaneous quantitation of platelet-bound immunoglobulin (IgG) and complement (C3) employing an enzyme-linked immunosorbent assay (ELISA) procedure. *Br. J. Haematol.* 44, 281-290.
 9. Johnstone A. and Thorpe, R. (1982). *Immunochemistry in Practice*, 57-59, Blackwell Scientific Publications, London.
 10. Conradie J.D., Govendor, M. and Visser, L. (1983). ELISA solid phase: partial denaturation of coating antibody yields a more efficient solid phase. *J. Immunol. Meth.* 59, 289-299.
 11. Grau, G.E., Piguet, P.-F., Gretener, D., Vesin, C. and Lambert, P.H. (1988). Immunopathology of thrombocytopenia in experimental malaria. *Immunol.* 65, 501-506.
 12. Mcmillan, R. (1983). Immune thrombocytopenia. *Clinics in Haematology.* 12, 69-88.
 13. Hymes, K., Shulman, S. and Karparkin, S. (1979). A solid phase radioimmunoassay for bound anti-platelet antibody. Studies on 45 patients with autoimmune platelet disorders. *J. Lab. Clin. Med.* 94, 639 - 648.

CHAPTER 5

ULTRASTRUCTURAL STUDIES OF ERYTHROCYTES INFECTED WITH Plasmodium falciparum.

5.1 INTRODUCTION

The erythrocyte membrane consists of a bilayer of phospholipids into which integral proteins are embedded. Peripheral proteins are bound by electrostatic interactions to the polar heads of phospholipids and/or to integral proteins. Most of the peripheral proteins are organized in a cytoskeletal network which underlies the cytoplasmic side of the membrane (1). Invasion of erythrocytes by malaria parasites results in modifications of the morphology and/or function of the host erythrocyte membrane including the lipid composition and fluidity (2). The concentration of fatty acids such as oleic and cis-vaccenic acids are increased whereas the concentration of arachidonic acid and cholesterol are decreased. The consequent increase in membrane fluidity affects the cytoskeleton-phospholipid interactions, leading to altered transport, enzymatic and osmotic properties of the host erythrocyte (2).

The invasion of the erythrocyte by a merozoite involves a series of complex interactions including recognition, attachment and membrane invagination (3). The invasive merozoite attaches to the erythrocyte by its apical end at which there is a pair of organelles called the rhoptries. Endocytosis is apparently induced by the secretion of a substance from the rhoptries that causes the erythrocyte to invaginate (4). After

internalisation, the parasite is surrounded by a parasitophorous vacuolar membrane (PVM) which is closely apposed to the parasite plasma membrane (3). Part of the PVM may originate from the erythrocyte membrane as evidenced by the reversal of the polarities of ATPase and NAD⁺-oxidase in the PVM in comparison to the erythrocyte membrane (2).

5.1.1 Parasite-induced changes to the erythrocyte membrane.

P. falciparum and *P. ovale*-infected erythrocytes exhibit protrusions or knobs on the surface of the erythrocyte membrane (6). The knobs are electron-dense, conically shaped and measure 90-100nm in diameter and 30-40nm in height. Although there is much controversy surrounding this point, it is commonly believed that the knobs are proteins of parasitic origin which increase in number as the intracellular parasites matures (7). It has also been observed that the distribution of knobs on the surface of the infected cell is not random, implying that they are inserted into specific domains of the erythrocyte membrane. Not all strains of *P. falciparum* produce knobs on the erythrocyte surface and some strains have been shown to lose this ability after lengthy periods of *in vitro* culturing (8).

5.1.2 Intra-erythrocytic cytoplasmic organelles.

The presence of numerous membrane-bounded organelles in the cytoplasm of infected erythrocytes suggests a mechanism for the exchange of material between the parasite and erythrocyte membranes. Aikawa *et al.* (9) identified the following structures in the cytoplasm of infected erythrocytes by transmission electron microscopy (TEM).

(i) **Maurer's cleft.** These structures are exceedingly diverse in shape but all consist of a unit membrane-bounded vesicle containing lumen of a low density. The vesicle is often elongated but it can also appear as a horse shoe or a circle presumably, representing, different cross sections of the same organelle. Maurer's clefts occur in both knob and knobless clones of *P. falciparum* parasites (7).

(ii) **Maurer's cleft with electron-dense material.** Maurer's clefts with electron-dense material on the cytoplasmic face of the unit membrane are only seen in *P. falciparum*-infected erythrocytes (early to late-throphozoite stage) that exhibit knobs. The electron-dense material on these clefts is roughly 100 nm in diameter and is identical in shape, size and electron density as the material seen under knobs (7).

(iii) **Golgi-like membrane stack.** Membrane stacks of between 5 and 15 elongated vesicles, each demarcated by a single unit membrane, were observed inside the cytoplasm of knob-producing, *P. falciparum*-infected erythrocytes. Each vesicle is aligned roughly parallel to adjacent members on each side of the stack. The lumen of the vesicle within the membrane stack is of low density, i.e. identical to Maurer's clefts. It is unknown if these stacks perform similar functions as the Golgi apparatus found in other cells (7,9). The different structures of cytoplasmic organelles are illustrated in Fig. 5.1.

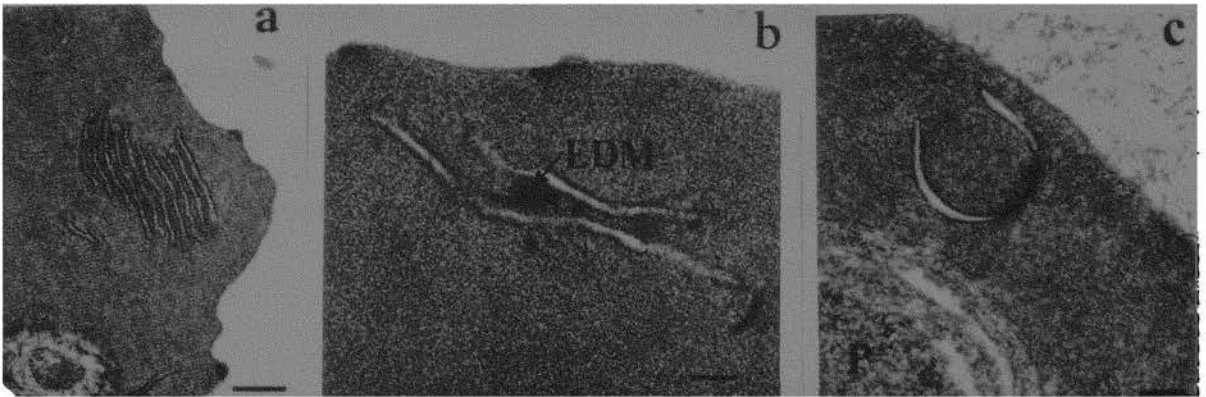


Figure 5.1 Transmission electron micrographs of organelles seen in the cytoplasm of infected erythrocytes. (a) Golgi membrane-like stack. Bar = 0.25 μm . (b) Maurer's clefts with electron dense material. Bar = 0.5 μm . (c) Maurer's cleft. Bar = 0.25 μm . Reproduced from (7).

5.1.3 Fixation of tissues for electron microscopy.

The high resolution obtainable with the electron microscope, necessitates that great care be taken with fixation procedures in order to preserve ultrastructural detail. Ideally, tissues used for microscopy should be preserved with chemicals that stabilize cellular structures as near as possible to the *in vivo* situation. However, this is only achievable within certain limits due to the high water content of biological materials (10). Fixation with buffered glutaraldehyde solution followed by buffered osmium tetroxide (OsO_4), is a standard procedure used for fixation of biological materials for electron microscopical studies (11).

Neither osmium tetroxide nor glutaraldehyde alone is suitable as a general fixative (11). Fixation with glutaraldehyde which crosslinks the amino

groups of proteins, seems to be superior to OsO_4 for the preservation of membrane proteins (10). By using OsO_4 alone more than 40% of the membrane protein content can be extracted compared to 10% after glutaraldehyde fixation. Fixation with glutaraldehyde alone does not prevent extraction of lipids by organic solvents during pre-embedding procedures (10). Loss of cholesterol and phospholipid from the erythrocyte membrane is prevented by the inclusion of a secondary fixation with OsO_4 ,

Glutaraldehyde may react with amino groups in different ways depending on its concentration and that of the protein in the tissue as well as the temperature and pH during fixation (10). The temperature and pH of the fixation solution may influence the penetration and crosslinking rate of glutaraldehyde. The fixative should have the same tonicity as the cell to prevent water depletion or engorgement and ultrastructural changes (13). Coetzee *et al.* (11) found that the best results were obtained with 2-3 % (v/v) glutaraldehyde in phosphate buffer (pH 7.4). Penman *et al.* (12) have shown that the discoid shape of erythrocytes is better preserved when low concentrations of glutaraldehyde are stepwise added to suspensions of guinea pig erythrocytes with a hematocrit higher than 20 % (v/v).

5.1.4 Ultrastructural features of erythrocyte-stage parasites.

i) *Merozoites*. They are oval-shaped, 1,5 μm in length and 1 μm in diameter. Common organelles include a nucleus, rhoptries and micronemes which are bound by a pellicular complex consisting of an outer and two inner membranes. The outer membrane is about 7.5 nm thick in comparison to

the 15 nm of the fenestrated inner membranes. The outer membrane is covered with a proteinaceous surface coat with a thickness of approximately 20 nm. Although the function of the coat is not yet fully understood, it appears to play a role in the immune evasion strategy of the extracellular merozoite (13). The apical end of the merozoite is cone-shaped and displays two electron dense rhoptries, each forming a duct which extends to the tip of the apical end (15).

ii) **Uninucleate trophozoites.** Upon invasion of erythrocytes, the surface coat is shed and merozoites changes from oval to round and finally to irregular shaped parasites. The latter phenomenon is apparently due to the rapid degradation of the inner membranes and the microtubules of the pellicular complex (15). Once these structures are removed the parasite is only surrounded by a single plasma membrane and a PVM which at least partially originated from the host erythrocyte (15). Some trophozoites show prominent ameboid activity producing extensions and invaginations of the parasite cytoplasm. Ring forms seen in the early development stages of the trophozoite appear to result from extensions of the parasite cytoplasm.

Aikawa *et al.* (15) have shown that the host cytoplasm is invaginated through a circular structure in the pellicle which they named a cytosome. After invagination of cytoplasm through the cytosome and digestion in food vacuoles, hemozoin or pigment derives from digested hemoglobin. When sections of mammalian malaria parasites are stained with a high pH solution such as lead citrate, the pigment particles are dissolved leaving a clear area where they were previously located (16).

Although it was previously believed that *P. falciparum* did not contain mitochondria, Fry and Beesley (17) recently isolated these organelles from trophozoite stages of the parasite. Ribosomes are abundant in the trophozoites and are mostly in the free form. The nucleus contains a high percentage of euchromatin suggesting that the nucleus is undergoing preparation for nuclear division (13).

iii) *Schizonts*. They are defined as parasites containing more than one nucleus and are larger than merozoites and uninucleate trophozoites. During nuclear division considerable morphological changes are observed, starting with the formation of spindle fibers in the nucleus. Mitochondria increase in size and become irregular in shape, due to the formation of several buds before finally undergoing fission to yield many mitochondria. The cytoplasmic organelles surrounded by an outer and two inner membranes are formed next. The area covered by the inner membranes protrude outwards into the parasitophorous vacuole space to form new merozoites. As the merozoites grow and develop, the original schizont decreases in size until only a small residual body containing malaria pigment particles, finally remains (13,17)

5.1.5 Objectives.

The objectives of the study were firstly to identify by light microscopy the species of *Plasmodium* to which isolate PfUP1 belongs. The second objective was to compare the results obtained with two different fixation procedures with each other and to those in the literature in order to select the most suitable procedure for electron microscopy.

5.2 MATERIALS AND METHODS

5.2.1 Parasite collection and *in vitro* culturing.

Malaria-infected erythrocytes were collected from a black resident of Giyani, North-Eastern Transvaal by venipuncture into acid citrate dextrose collection tubes (Medical Home and Nursing Supplies, Pretoria). An *in vitro* continuous culture was initiated from cryopreserved blood as described in Chapter 3 (isolate PfUP1).

5.2.2 Preparation of blood smears for light microscopy.

Thin smears from *in vitro* cultures of PfUP1 on microscope slides were fixed and stained with Giemsa as described in Chapter 2. The blood smears were examined with a Nikon light microscope and photographed using Kodak Ectachrome 400 colour film.

5.2.3 Slow fixation of infected erythrocytes.

Erythrocytes were collected by centrifugation of an unsynchronized culture of PfUP1 at 1000 g for 5 minutes. The erythrocyte pellet was washed twice with RPMI 1640 without serum and diluted afterwards to 20 % hematocrit using the same medium. The erythrocyte suspension (2 ml) was cooled to 4°C and 10µl of a 2,7 % (v/v) glutaraldehyde solution (Poloron, Bio-rad) in 0,07M sodium phosphate buffer, pH 7,4 was slowly added to the erythrocyte suspension and mixed by gentle agitation. The addition of glutaraldehyde was repeated every hour for a total of ten hours. The final concentration of glutaraldehyde was 0,13 % (v/v). The cell suspension was incubated for a further 2 hours at 4 °C before the cells were processed for scanning and transmission electron microscopy.

5.2.4 Fast fixation of infected erythrocytes.

Erythrocytes were obtained from an unsynchronized culture and washed as above. The pellet was resuspended in RPMI 1640 without serum to give a 50 % hematocrit. The erythrocytes were fixed at room temperature by adding 1ml of a 2,5 % (v/v) glutaraldehyde solution (0,07M sodium phosphate buffer, pH 7.4) to 4 ml erythrocyte suspension. Fixation was carried out for 2 hours before the fixed erythrocytes were processed for scanning and transmission electron microscopy.

5.2.5 Processing of glutaraldehyde-fixed tissues for scanning electron microscopy.

Fixed erythrocyte pellets (400 μ l) were suspended in 2 ml 0,07M sodium phosphate buffer, pH 7.4, and collected by filtration on a Whatman GF/A filter. After filtration the filters were placed in 1 % (v/v) OsO₄ for 1h. Dehydration was done by placing the filter with fixed erythrocytes for 10 minutes each in 30 %, 50 %, 70 %, 100 % (v/v) and absolute acetone. The samples were critically dried using liquid carbon dioxide and sputtered with gold. Non-infected cells were treated similarly to infected cells and used as controls. Fixed preparations were inspected with a Jeol JSM 840 scanning electron microscope operating at 12 kV and photographs were taken on ASA 125, Ilford FP4 film.

5.2.6 Processing of glutaraldehyde-fixed, infected tissues for transmission electron microscopy.

Fixed erythrocytes were suspended in 10 % (w/v) bovine serum albumin in 0,07M sodium phosphate buffer, pH 7.4 and placed in a 1,8 ml plastic Eppendorf tube. The erythrocytes were centrifuged at 8000 x g for 1 min and the excess solution, except for a 2 mm layer of albumin-buffer

on top of the erythrocytes, was aspirated. The tube was then slowly filled with 2.5 % (v/v) glutaraldehyde (1 ml) in 0.07M phosphate buffer, pH 7.4, without disturbing the erythrocytes. After incubation for 12 hours at 20 °C the albumin-embedded erythrocyte pellet was removed from the Eppendorf tube and cut into approximately one mm blocks. After post-fixation in 1 % (v/v) OsO₄ for 1 hour at 20 °C, the blocks were dehydrated by sequential treatment with 40 %, 60 %, 80 %, 90 % and 100 % acetone (5 min/step). Final embedding was in Quetol, which was prepared as follows:

Table 5.1 Quetol embedding resin. The first four components were mixed thoroughly before S1 was added.

Reagent	Mass
1. Quetol	3,90 g
2. Nadic Methyl Anhydrate (NMA)	4,46 g
3. Dodecyl Succinic Anhydrate (DDSA)	1,66 g
4. Araldite Cy212 resin (RD2)	0,20 g
5. Di-ethyl amino ethanol (S1)	0,10 g

Bovine serum albumin-embedded erythrocytes were incubated for 12 hours in Quetol embedding medium at 20 °C to allow infiltration of the tissue. The resin was polymerized in an oven at 60 °C for 48 hours before being cut into 70-100 nm sections on a Reichert Jung Ultracut E microtome, equipped with a diamond knife. The thin sections were mounted on G200 copper grids and contrasted with uranyl acetate (4%) and Reynolds lead citrate (18). Thin sections were inspected in a Philips EM301 transmission electron microscope operated at 60kV.

5.3 RESULTS

5.3.1 Light microscopy of PfUP1-infected erythrocytes.

The four species of malaria parasites which infects man differ with respect to their physiology and pathology but are best characterized on the basis of their morphology.

Three of the four blood stages of isolate PfUP1 are shown in Fig. 5.2. Typical *P. falciparum* parasites i.e. small rings, consisting of two red chromatin masses and a thin blue-coloured cytoplasm are present. The trophozoites are round and infected erythrocytes are the same colour and size as the non-infected erythrocytes. The schizonts rosetted around masses of haemozoin pigment and consists of 18-20 merozoites each.

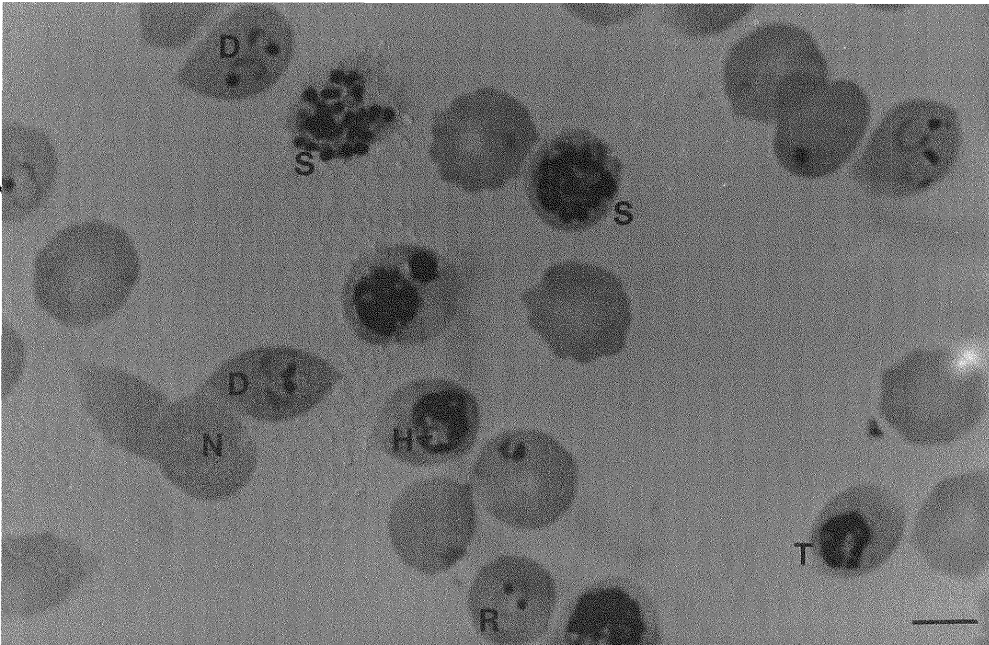


Figure 5.2 Light microscope photograph of the blood stages of isolate PfUP1. A thin blood smear was made from a continuous culture and stained with Giemsa. Blood smears were viewed under a Nikon light microscope using the 100 magnified oil immersion lens. D-double infection, H-haemozoin-pigment granules, N-normal erythrocyte, R-rings, S-schizont, T-trophozoite. (Bar = 7.5 μm .)

5.3.2 Scanning electron microscopy of PFUP1-infected erythrocytes.

Non-infected erythrocytes controls fixed by the slow method, are shown in Figure 5.3.. In the non-infected culture 95 % of the erythrocytes observed were discocytes.

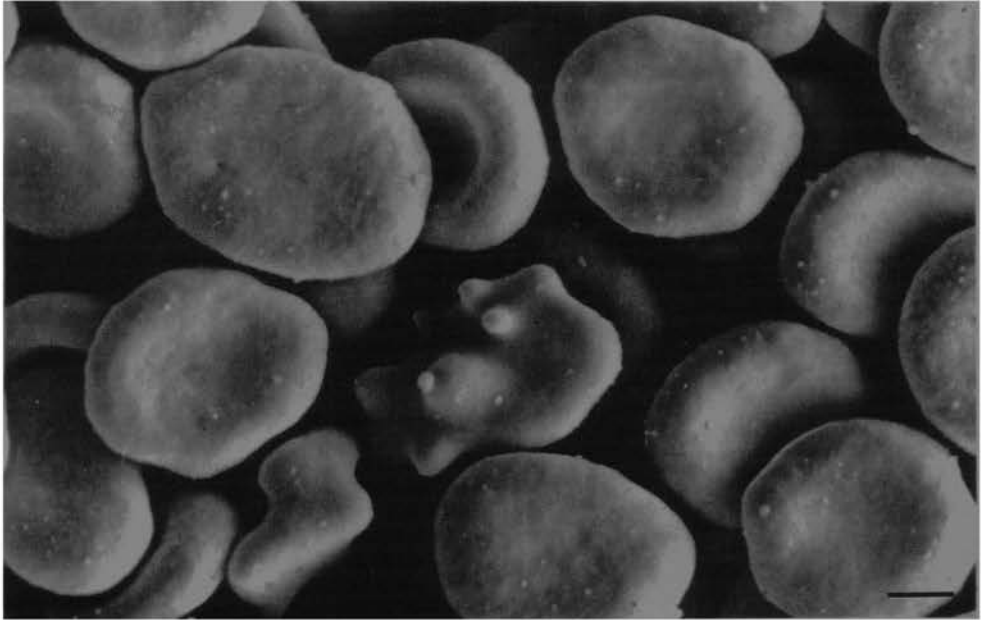


Figure 5.3 Scanning electron micrograph of non-infected erythrocytes after four days in continuous culture. The blood sample was fixed using the slow glutaraldehyde method (See text) (Bar = 2.8 μ m.)

Scanning electron micrographs of PfUP1-infected erythrocytes fixed with the slow method, are shown in Fig. 5.4 (a) and (b).

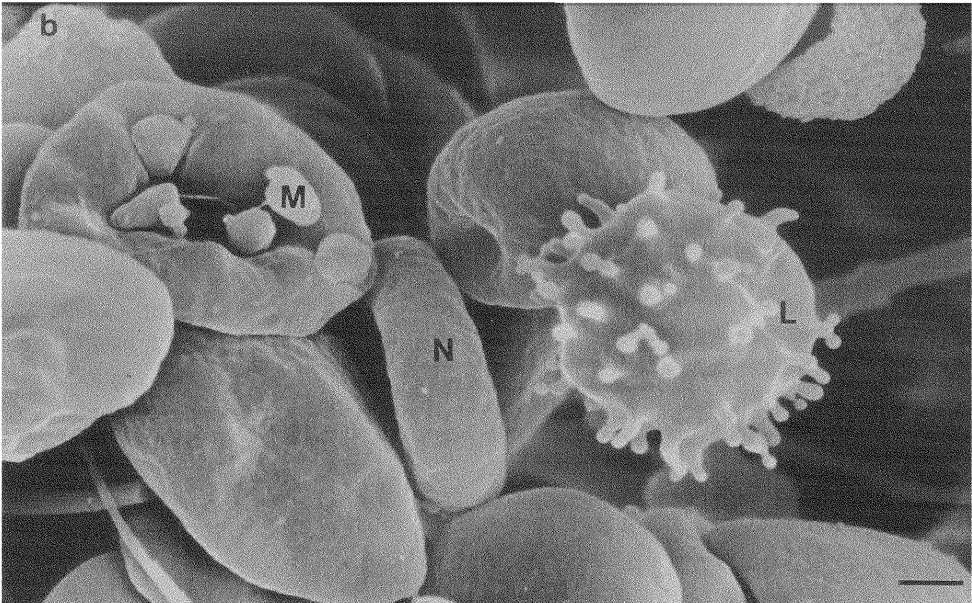
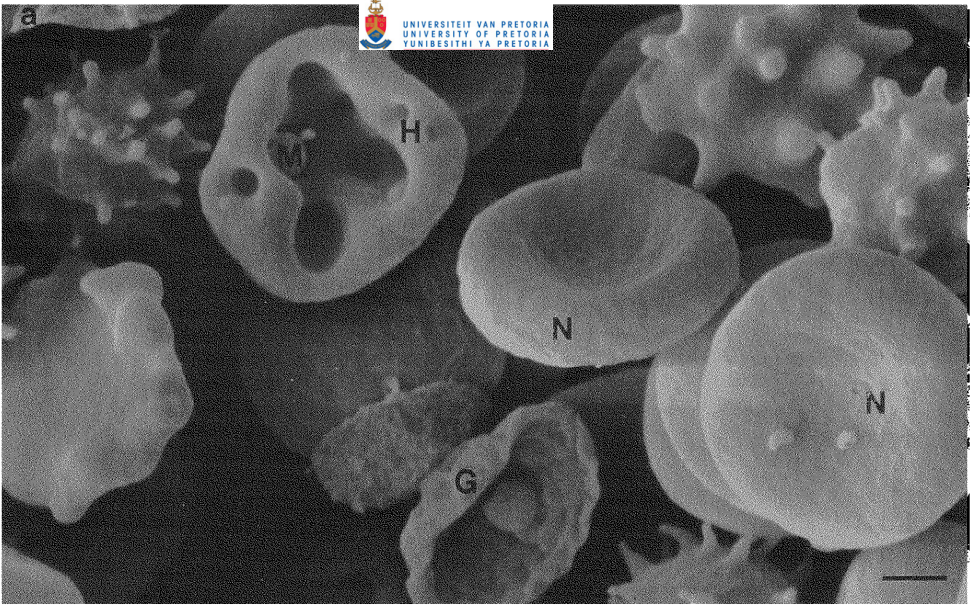


Figure 5.4 Scanning electron micrograph of PfUP1-infected erythrocytes fixed with the slow glutaraldehyde method. H-holes, M-merozoite, N-normal erythrocyte, L-lymphocyte, G-erythrocyte ghost. (a) Bar = 2.5 μm . (b) Bar = 2.0 μm .

The erythrocyte in Fig. 5.4 (a) is distorted and has invaginations as well as a single merozoite which is attached to the surface. A discocyte and echinocyte are also present in the same frame. In Fig. 5.4 five

merozoites are attached to a distorted erythrocyte. A lymphocyte is also present in the same micrograph.

Scanning electron micrographs of PfUP1-infected erythrocytes after fixation with the fast method are shown in Fig. 5.5.

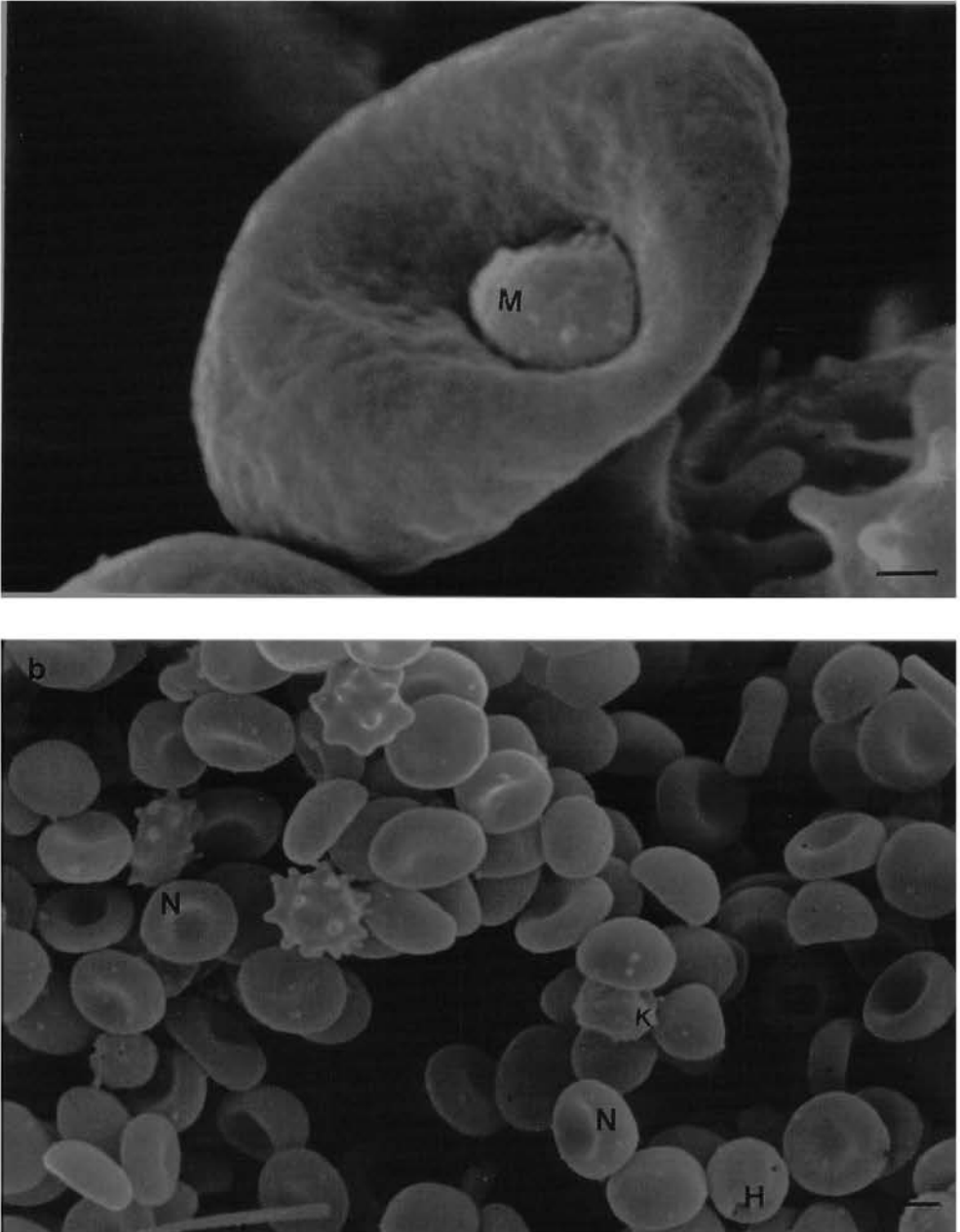


Figure 5.5 Scanning electron micrograph of PfUP1-infected erythrocytes fixed by the fast method (see text for details). (a) Shows a merozoite attached to an erythrocyte. (b) Infected erythrocytes shown at a lower magnification. N-normal erythrocyte, M-merozoite, H-holes, K-knobs. (a) Bar = 0.5 μ m. (b) Bar = 10 μ m.

In (a) a merozoite is shown attached to an erythrocyte. It is evident that most of the erythrocytes in (b) are discocytes when viewed at a low magnification. Erythrocytes with knobs (K) and another with holes (H) can also be discerned. Numerous holes with variable sizes from around 50 to 300 nm in diameter were observed during this study. The control fixed with the fast method (not shown) was identical to the control fixed with the slow method (Fig. 5.3), ie. no holes were observed.

Knobs were observed in PfUP1-infected erythrocytes which were fixed with either the slow or fast methods. Knob sizes were randomly determined from infected erythrocytes which were fixed with the slow method (Fig. 5.6). The mean value was 165.4 ± 16 nm ($n = 15$).

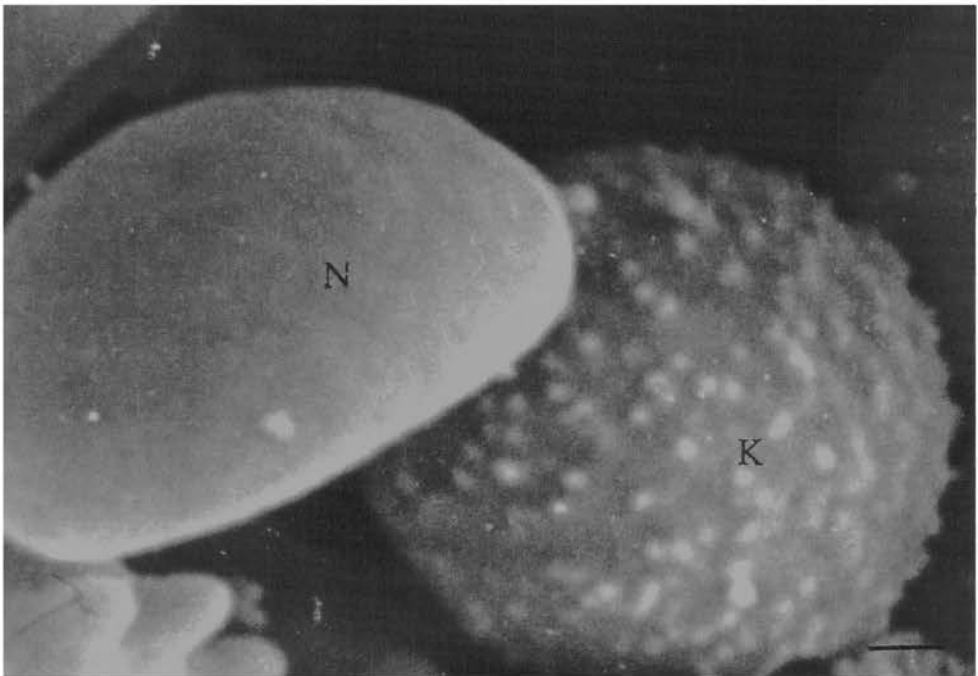


Figure 5.6 Scanning electron microscope photographs of PfUP1-infected erythrocyte with knobs. The blood sample was fixed by the slow method and processed as described in the text. N-normal erythrocyte, K-knob presenting erythrocyte. (Bar = 0.5 μ m.)

5.3.3 Transmission electron microscopy of PfUP1-infected erythrocytes.

Transmission electron micrographs of erythrocytes infected with PfUP1 are shown in Fig. 5.7

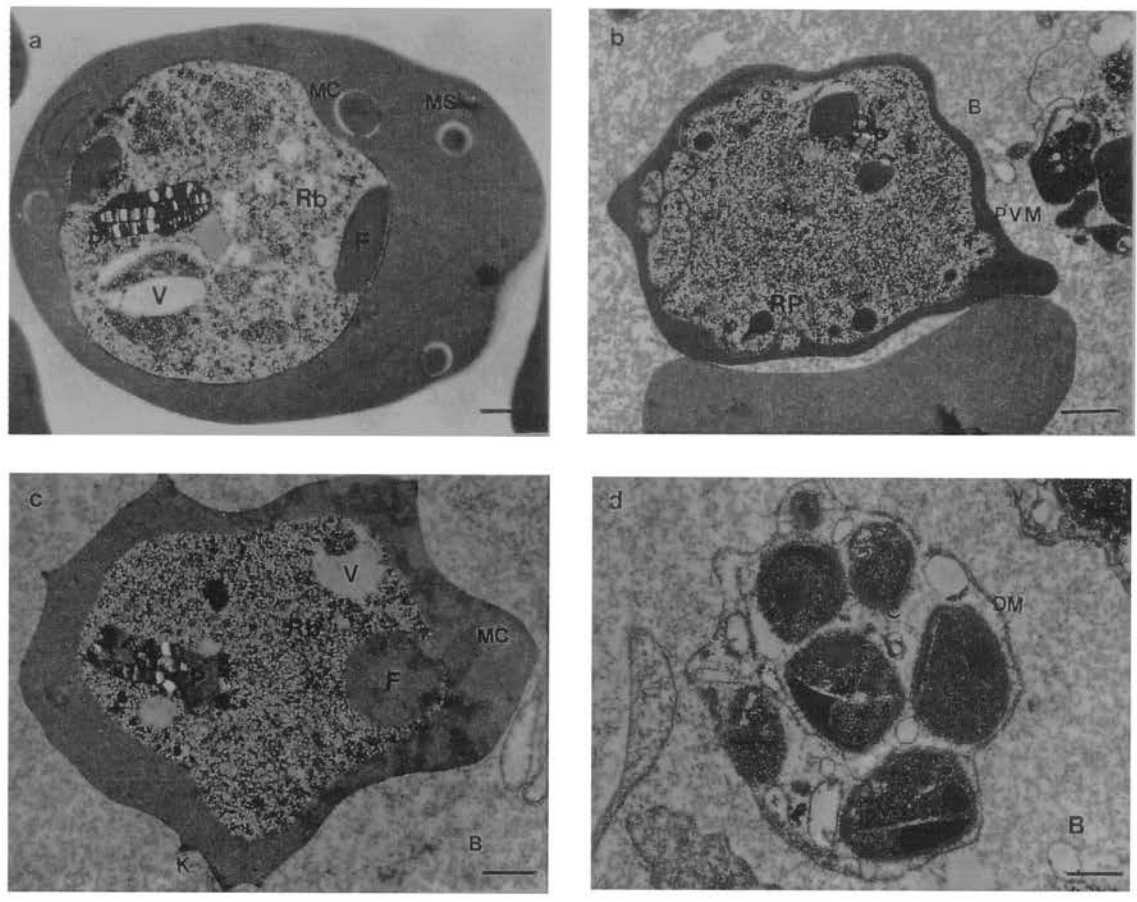


Figure 5.7 Transmission electron micrographs of PfUP1-infected erythrocytes. (a) fixed using the slow glutaraldehyde method; (b), (c) and (d) were fast fixed using 1 % glutaraldehyde solution. (b), (c) and (d) were imbedded using bovine serum albumin as supporting medium. B-background-glutaraldehyde fixed albumin, C-merozoite coat DM-double membrane, F-food vacuole, P-pigment granules, K-knobs, MC-Maurer's cleft, MS-membrane stacks, R-Rhoptry in merozoite, Rb-ribosomes, N-nucleus PVM-parasitophorous vacuolar membrane. V-Vacuole. RP-rhoptry precursors.

(a) Bar = 0.4 μm (b) Bar = 0.5 μm (c) Bar = 0.4 μm (d) Bar = 0.5 μm

Trophozoites lack organelles normally seen in merozoites (rhoptries, micronemes, pellicular complex) but contain pigment granules and food vacuoles, and are uninucleate (a and c). The membranes in (a) are less well defined compared to (b), (c) and (d), eg. the PVM is not visible. The cytoplasm of the host erythrocyte in (a) contains organelles which are similar to Maurer's clefts and Maurer's clefts with electron dense material. Trophozoites are also irregular in shape and their ameboid activity produces invaginations and extensions of the parasite and the erythrocyte cytoplasm. In (b) an early schizont is shown having only a few rhoptries since the division of the nucleus is not yet complete. Oval-shaped merozoites measuring 1.5 μ m in length, with rhoptries, micronemes and a pellicular complex are present at the late schizont stage (d).

5.4 DISCUSSION

The presence of malaria parasites in a patient's blood is detected by light microscopy using either thick or thin blood smears stained with Giemsa. Only ring stages are observed in the peripheral blood of patient's infected with *P. falciparum* since erythrocytes infected with trophozoites or schizonts of this species (7) adhere to the epithelial cells of blood vessels.

Isolate PfUP1 could be identified as *P. falciparum* based on the following observations (Fig. 1.4, 5.2): Extracellular trophozoite and schizont stage parasites which only occur in *P. vivax* infections, were absent. Infected erythrocytes are the same size, colour and shape as non-infected

erythrocytes which excluded *P. vivax* and *P. ovale* whereas the absence of band-shaped trophozoites also excluded *P. malariae*. Ring-stage parasites contained two chromatin dots which are typical for *P. falciparum*.

Erythrocytes with holes were observed after fixation with both slow and fast methods (Fig. 5.4 and 5.5). Kreier *et al.* (4) demonstrated up to 4 holes in erythrocytes infected with different species of malaria parasites which he concluded: "appears to be associated with multiple merozoite infections". However, in our study up to 8 holes were sometimes observed after fixation with either the slow or fast methods. These many holes are unusual but could be caused by merozoites leaving partly fixed erythrocytes which are unable to reseal and/or merozoites attempting to enter partly fixed erythrocytes which is still flexible but not amenable to invasion.

Wild isolates of *P. falciparum* usually contain more than one strain of which some may be of the knobless variety (8). Although knobs were seen on some of the erythrocytes infected with isolate PfUP1, no correlation was attempted with the parasitemia to establish the proportion of knob-producing parasites, since an unsynchronized culture was used. The knob sizes (165.4 ± 16 nm) in our study (Fig. 5.6) agree with that of the trophozoite-containing erythrocytes reported by Gruenberg *et al.* (diameter, 110-160 nm; 18) since the Knob sizes in schizont-bearing erythrocytes varied between 70-100 nm (18).

Parasites in Fig. 5.7 (a) and (c) can be identified as trophozoites due to the absence of typical merozoite intracellular organelles, their irregular shape and uninucleate character as well as the presence of food vacuoles with their associated hemozoin crystals. The parasite in Fig. 5.7(d) is

typical of merozoites which contain rhoptries, nucleus, mitochondria and is covered by a surface coat. The parasite in Fig. 5.7(b) displays many small rhoptries and is in the process of dividing, but fully developed merozoites are not present. The parasite is larger than a merozoite or an uninucleate trophozoite and is therefore at the schizont development stage.

Comparisons between the transmission electron micrographs in Fig 5.7 revealed the following: The trophozoite in (a) which was fixed using the slow method, displays Maurer's clefts and membrane stacks in the erythrocyte cytoplasm. Inside the trophozoite haemozoin pigment, food vacuoles and low electron dense-containing vacuoles can be discerned. However, the membranes appear to be undefined and rather fuzzy.

The trophozoite in (c) which were fixed using the fast method also displays Maurer's clefts in the erythrocyte cytoplasm and the same structures inside the parasite as seen with the slow fixation method. Knob-presenting and knobless erythrocytes were seen in both methods of fixation. The major difference between the slow and fast fixation method appears to be that the membranes are better preserved in the latter method. For instance, the PVM and pellicular complex can be clearly discerned in Fig. 5.7 (b and d) but not in (a).

Most of the fine structure of the parasite appears to have been lost using the slow fixation method, which makes the fast fixation method superior. The lack of membrane preservation with the former method may be due to a loss of unfixed soluble membrane components during the prolonged fixation or the acetone treatment (11).

Thus, the PfUP1 isolate is of the *P. falciparum* strain and could be a mixture of isolates of which some may have the ability to produce knobs and others not. The same cytoplasmic organelles as described in the literature were observed in our infected erythrocytes. Both fixation methods can be used for scanning electron microscopy, but when transmission electron microscopical examination is needed, the fast fixation method yielded better preservation of membranes.

5.5 REFERENCES

1. Atkinson C.T. and Aikawa M. (1987). Ultrastructural location of erythrocyte cytoskeletal and integral membrane proteins in *Plasmodium falciparum* infected erythrocytes, *Europ. J. Cell. Biol.* 45, 192-199.
2. Sherman I.W. (1985). Membrane structure and function of malaria parasites and the infected erythrocyte. *Parasitology*, 91, 609-645.
3. Trager W. (1986). Modification of host cells produced by intracellular Protozoa. In: *Living together: the biology of animal parasitism.* 209-226, Plenum Press, New York.
4. Kreier J.P. Taylor W.M. and Wagner W.M. (1972). Destruction of erythrocytes in monkeys infected with *P. cynomolgio*, *Am. J. Vet. Res.* 33, 409-414.
5. Perkins M.E. (1989). Erythrocyte invasion by the malarial merozoite: Recent advances. *Exp. Parasit.* 69, 94-99.
6. Langreth S.G. and Jensen J.B. (1978). Fine structure of human malaria *in vitro*. *J. Protozool* 25, 443-452.
7. Kilejian A. (1979). Characterization of a protein correlated with the production of knoblike protrusions on membranes of erythrocytes infected with *Plasmodium falciparum* *Proc Nat Acad Sci USA* 76, 4650-4653.

8. Langreth S.G., Reese R.T., Motyl M.R. and Trager W. (1979). *Plasmodium falciparum* : Loss of knobs on the infected erythrocyte surface after long-term cultivation. *Exp. Parasitol.* 48, 213-219.
9. Aikawa M., Andrutis A.T. and Howard R.J. (1986). Membrane-associated electrondense material of the asexual stages of *Plasmodium falciparum* : Evidence for movement from the intracellular parasite to the erythrocyte membrane. *Am J Trop Med Hyg.* 35, 30-36.
10. McMillan P.N. and Luftig R.B. (1973). Preservation of erythrocyte ghost ultrastructure achieved by various fixatives. *Proc Nat Acad Sci USA.* 70(11), 3060-3064.
11. Coetzee J. and Van der Merwe C.F. (1986). The influence of processing protocol on the ultrastructure of bean leaf cells. *S. Afr. Tydskrif vir Wetenskap.* 52, 95-99.
12. Penman K.M., Lawton J., Visser L. and Louw A.I. (1988). Fixation with glutaraldehyde of suspensions of isolated guineapig erythrocytes for scanning electron microscopy. *S. Afr. Tydskrif vir Wetenskap.* 84, 133-136.
13. Garnham P.C.C. (1984). Life cycles. In: Handbook of experimental pharmacology, Vol 68. (Eds W. Peters and W.A.G. Richards) 3-28, Springer-verlag, Berlin.
14. Kreier J.P., Seed T.M., Mohan R. and Pfister R. (1972). *Plasmodium* spp.: The relationship between erythrocyte morphology and parasitasion in chicken, rats and mice. *Exp parasitol.*, 31, 19-28.

15. Reynolds E.S. (1963) The use of lead citrate at high pH as an electron-opaque stain in electron microscopy. *J Cell Biol.* 17, 208-221.
16. Aikawa, M. (1971). *Plasmodium*: The fine structure of malarial parasites. *Exp. Parasitol.* 30, 284-320.
17. Fry M. and Beesley J.E. (1990). Mitochondria of *Plasmodium* species. *Parasitology* 102, 17-26.
18. Gruenberg J., Allred D.R. and Sherman I.W. (1983). Scanning electron microscope-analysis of the protrusions (knobs) present on the surface on *Plasmodium falciparum*-infected erythrocytes. *J. Cell Biol.* 97, 795-802.
19. Fripp P.J. (1983). In: An introduction to human parasitology. Vol 2., Macmillan, South Africa.